

**Gaps between jets at hadron colliders in the next-to-leading BFKL framework**F. Chevallier,<sup>1,\*</sup> O. Kepka,<sup>1,2,3,†</sup> C. Marquet,<sup>4,5,‡</sup> and C. Royon<sup>1,§</sup><sup>1</sup>*IRFU, Service de physique des particules, CEA, Saclay, 91191 Gif-sur-Yvette cedex, France*<sup>2</sup>*IPNP, Faculty of Mathematics and Physics, Charles University, Prague, Czech Republic*<sup>3</sup>*Center for Particle Physics, Institute of Physics, Academy of Science, Prague, Czech Republic*<sup>4</sup>*Institut de Physique Théorique, CEA, Saclay, 91191 Gif-sur-Yvette cedex, France*<sup>5</sup>*Department of Physics, Columbia University, New York, New York 10027, USA*

(Received 26 March 2009; published 20 May 2009)

We investigate diffractive events in hadron-hadron collisions, in which two jets are produced and separated by a large rapidity gap. In perturbative QCD, the hard color-singlet object exchanged in the  $t$  channel, and responsible for the rapidity gap, is the Balitsky-Fadin-Kuraev-Lipatov Pomeron. We perform a phenomenological study including the corrections due to next-to-leading logarithms. Using a renormalization-group improved next-to-leading logarithmic kernel, we show that the Balitsky-Fadin-Kuraev-Lipatov predictions are in good agreement with the Tevatron data and present predictions which could be tested at the LHC.

DOI: 10.1103/PhysRevD.79.094019

PACS numbers: 13.87.-a, 12.38.Bx

**I. INTRODUCTION**

The discovery of diffractive interactions in hard processes at hadron colliders has triggered a large effort devoted to understand rapidity gaps in processes with a hard scale. Since events with a gap between two jets were observed in  $p\bar{p}$  collisions at the Tevatron about 10 yr ago [1], many theoretical works have investigated these processes in QCD. While describing diffractive processes in QCD has been a challenge for many years, one should be able to understand hard diffractive events with perturbative methods.

In a hadron-hadron collision, a jet-gap-jet event features a large rapidity gap with a high- $E_T$  jet on each side ( $E_T \gg \Lambda_{\text{QCD}}$ ). Across the gap, the object exchanged in the  $t$  channel is color singlet and carries a large momentum transfer, and when the rapidity gap is sufficiently large, the natural candidate in perturbative QCD is the Balitsky-Fadin-Kuraev-Lipatov (BFKL) Pomeron [2]. Of course the total energy of the collision  $\sqrt{s}$  should be big ( $\sqrt{s} \gg E_T$ ) in order to get jets and a large rapidity gap.

To compute the jet-gap-jet process in the BFKL framework, the problem of coupling the BFKL Pomeron to partons, instead of colorless particles in the standard approach, has to be solved first. Indeed, one usually uses the fact that impact factors vanish when hooked to gluons with no transverse momentum, a property of colorless impact factors. For instance, this is what allows the Feynman diagram calculation to turn into a conformal invariant Green function [3]. However, with colored particles, this BFKL Green function cannot be used and should be modi-

fied accordingly. The Mueller-Tang (MT) prescription [4] is widely used in the literature.

On the phenomenological side, the original MT calculation is not sufficient to describe the data. A first try to improve it was attempted [5] by also taking into account the soft interactions which in hadron-hadron collisions can destroy the rapidity gap. An agreement was only obtained if the leading-logarithmic (LL) BFKL calculation was done with a fixed value of the coupling constant  $\alpha_s$ , which is not satisfactory. Moreover, it is also known that next-to-leading logarithmic (NLL) BFKL corrections can be large. In [6], it was shown that a good description of the data could be obtained when some NLL corrections were numerically taken into account in an effective way [7], but the full NLL-BFKL kernel [8] could still not be implemented. As a result, these tests on the relevance of the BFKL dynamics were not conclusive.

On the theoretical side, it is known that NLL corrections to the LL-BFKL predictions can be large due to the appearance of spurious singularities in contradiction with renormalization-group requirements. However, it has been realized [9,10] that a renormalization-group improved NLL regularization can solve the singularity problem and lead to reasonable NLL-BFKL kernels (see also [11] for different approaches). This motivates our phenomenological study of jet-gap-jet events in the NLL-BFKL framework. One goal is to motivate further measurements at the Tevatron and the LHC.

Such NLL-BFKL phenomenological investigations have been devoted to the proton structure function [12], forward-jet production in deep inelastic scattering [13,14], and Mueller-Navelet jets in hadron-hadron collisions [15,16]. While for the structure function analysis the NLL corrections did not really improve the BFKL description, it was definitively the case in the forward-jet analysis, and they play a non-negligible role for the Mueller-Navelet

\* florent.chevallier@cea.fr

† kepka@fzu.cz

‡ cyrille@phys.columbia.edu

§ royon@hep.saclay.cea.fr

jet predictions. Therefore, it is natural to investigate what happens for jet-gap-jet events and what is the magnitude of the NLL corrections with respect to the LL-BFKL results for this observable.

The plan of the paper is the following. In Sec. II, we introduce the phenomenological NLL-BFKL formulation of the jet-gap-jet cross section. In Sec. III, we compare the LL- and NLL-BFKL calculations and confront them with the Tevatron measurements. In Sec. IV, we present predictions for the jet-gap-jet cross section at the LHC. We also discuss the dependence of our results with respect to the choice of the renormalization scale. Section V is devoted to conclusions and outlook.

## II. THE JET-GAP-JET CROSS SECTION IN THE BFKL FRAMEWORK

In a hadron-hadron collision, the production of two jets with a gap in rapidity between them is represented in Fig. 1, with the different kinematic variables. We denote  $\sqrt{s}$  the total energy of the collision,  $p_T$  and  $-p_T$  the transverse momenta of the two jets, and  $x_1$  and  $x_2$  their longitudinal fraction of momentum with respect to the incident hadrons as indicated on the figure. The rapidity gap between the two jets is  $\Delta\eta = \ln(x_1 x_2 s / p_T^2)$ . We write the cross section in the following form:

$$\frac{d\sigma^{pp \rightarrow XJJY}}{dx_1 dx_2 dp_T^2} = \mathcal{S} f_{\text{eff}}(x_1, p_T^2) f_{\text{eff}}(x_2, p_T^2) \frac{d\sigma^{gg \rightarrow gg}}{dp_T^2}, \quad (1)$$

where the functions  $f_{\text{eff}}(x, p_T^2)$  are effective parton distributions that resum the leading logarithms  $\log(p_T^2/\Lambda_{\text{QCD}}^2)$ . They have the form

$$f_{\text{eff}}(x, \mu^2) = g(x, \mu^2) + \frac{C_F^2}{N_c^2} (q(x, \mu^2) + \bar{q}(x, \mu^2)), \quad (2)$$

where  $g$  (respectively  $q, \bar{q}$ ) is the gluon (respectively quark, antiquark) distribution function in the incoming hadrons.

Even though the process we consider involves moderate values of  $x_1$  and  $x_2$  and the perturbative scale  $p_T^2 \gg \Lambda_{\text{QCD}}^2$ , which we have chosen as the factorization scale, the cross section (1) does not obey collinear factorization. This is due to possible secondary soft interactions between the colliding hadrons which can fill the rapidity gap. Therefore, in (1), the collinear factorization of the parton distributions  $f_{\text{eff}}$  is corrected with the so-called gap-

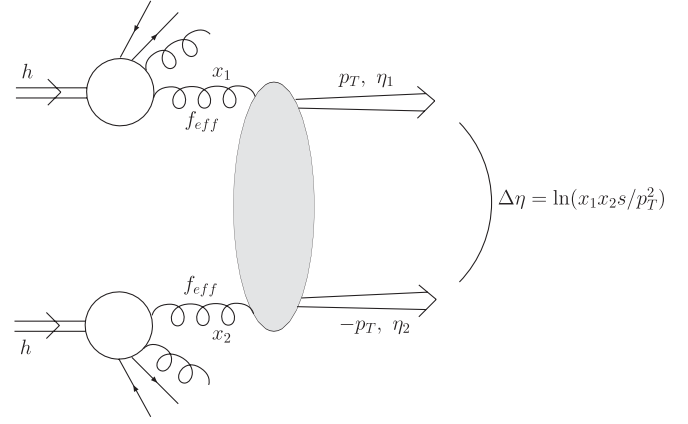


FIG. 1. Production of two jets separated by a large rapidity gap in a hadron-hadron collision. The kinematic variables of the problem are displayed.  $s$  is the total energy squared of the collision,  $p_T$  ( $\eta_1$ ) and  $-p_T$  ( $\eta_2$ ) are the transverse momenta (rapidities) of the jets, and  $x_1$  and  $x_2$  are their longitudinal momentum fractions with respect to the incident hadrons.  $\Delta\eta$  is the size of rapidity gap between the jets.

survival probability  $\mathcal{S}$ : since the soft interactions happen on much longer time scales, they are factorized from the hard part  $d\sigma^{gg \rightarrow gg}/dp_T^2$ . This cross section is given by

$$\frac{d\sigma^{gg \rightarrow gg}}{dp_T^2} = \frac{1}{16\pi} |A(\Delta\eta, p_T^2)|^2 \quad (3)$$

in terms of the  $gg \rightarrow gg$  scattering amplitude  $A(\Delta\eta, p_T^2)$ . The two measured jets are initiated by the final-state gluons, and we are neglecting possible hadronization effects.

In the following, we consider the high energy limit in which the rapidity gap  $\Delta\eta$  is assumed to be very large. The BFKL framework allows us to compute the  $gg \rightarrow gg$  amplitude in this regime, and the result is known up to NLL accuracy. Since in this calculation the BFKL Pomeron is coupled to quarks or gluons, the BFKL Green function cannot be used as it is and should be modified. The transformation proposed in [4] is based on the fact that one should recover the analyticity of the Feynman diagrams. It was later argued that their prescription corresponds to a deformed representation of the BFKL kernel that indeed could be coupled to colored particles and for which the bootstrap relation is fulfilled [17]. Applying the MT prescription at NLL leads to

$$A(\Delta\eta, p_T^2) = \frac{16N_c \pi \alpha_s^2}{C_F p_T^2} \sum_{p=-\infty}^{\infty} \int \frac{d\gamma}{2i\pi} \frac{[p^2 - (\gamma - 1/2)^2] \exp\{\bar{\alpha}(p_T^2) \chi_{\text{eff}}[2p, \gamma, \bar{\alpha}(p_T^2)] \Delta\eta\}}{[(\gamma - 1/2)^2 - (p - 1/2)^2][(\gamma - 1/2)^2 - (p + 1/2)^2]} \quad (4)$$

with the complex integral running along the imaginary axis from  $1/2 - i\infty$  to  $1/2 + i\infty$  and with only even conformal spins contributing to the sum [18]. The running coupling is given by

$$\bar{\alpha}(p_T^2) = \frac{\alpha_s(p_T^2) N_c}{\pi} = [b \log(p_T^2/\Lambda_{\text{QCD}}^2)]^{-1}, \quad (5)$$

$$b = \frac{11N_c - 2N_f}{12N_c}. \quad (6)$$

Let us give some more details on Eq. (4). The NLL-BFKL effects are phenomenologically taken into account by the effective kernels  $\chi_{\text{eff}}(p, \gamma, \bar{\alpha})$ . For  $p = 0$ , the scheme-dependent NLL-BFKL kernels provided by the regularization procedure  $\chi_{\text{NLL}}(\gamma, \omega)$  depend on  $\omega$ , the Mellin variable conjugate to  $\exp(\Delta\eta)$ . In each case, the NLL kernels obey a *consistency condition* [9] which allows us to reformulate the problem in terms of  $\chi_{\text{eff}}(\gamma, \bar{\alpha})$ . The effective kernel  $\chi_{\text{eff}}(\gamma, \bar{\alpha})$  is obtained from the NLL kernel  $\chi_{\text{NLL}}(\gamma, \omega)$  by solving the implicit equation  $\chi_{\text{eff}} = \chi_{\text{NLL}}(\gamma, \bar{\alpha}\chi_{\text{eff}})$  as a solution of the consistency condition.

In [15,16], the regularization procedure has been extended to nonzero conformal spins, and the kernel  $\chi_{\text{NLL}}(p, \gamma, \omega)$  was obtained from the results of [19]. The formulas needed to compute it can be found in the Appendix of [15] (in the present study we shall use the S4 scheme in which  $\chi_{\text{NLL}}$  is supplemented by an explicit  $\bar{\alpha}$  dependence; the results in the case of the S3 scheme are similar). Then the effective kernels  $\chi_{\text{eff}}(p, \gamma, \bar{\alpha})$  are obtained from the NLL kernel by solving the implicit equation:

$$\chi_{\text{eff}} = \chi_{\text{NLL}}(p, \gamma, \bar{\alpha}\chi_{\text{eff}}). \quad (7)$$

It is important to note that in Eq. (4), we used the leading-order nonforward quark and gluon impact factors. We point out that the next-to-leading-order impact factors are known [20], and that in principle a full NLL analysis is feasible, but this goes beyond the scope of our study.

By comparison, the LL-BFKL formula is formally the same as (4) with the substitutions

$$\begin{aligned} \chi_{\text{eff}}(p, \gamma, \bar{\alpha}) \rightarrow \chi_{\text{LL}}(p, \gamma) &= 2\psi(1) - \psi\left(1 - \gamma + \frac{|p|}{2}\right) \\ &\quad - \psi\left(\gamma + \frac{|p|}{2}\right), \\ \bar{\alpha}(k^2) \rightarrow \bar{\alpha} &= \text{const parameter}, \end{aligned} \quad (8)$$

where  $\psi(\gamma) = d \log \Gamma(\gamma) / d\gamma$  is the logarithmic derivative of the  $\Gamma$  function. In the NLL-BFKL formula, the value of  $\bar{\alpha}$  is imposed by the scale  $p_T^2$ . We shall later test the sensitivity of our results when using  $\lambda p_T^2$  and varying  $\lambda$  between 0.5 and 2; this is done using Eq. (4) with the appropriate substitutions [21]:

$$\begin{aligned} \bar{\alpha}(p_T^2) \rightarrow \bar{\alpha}(\lambda p_T^2) + b\bar{\alpha}^2(p_T^2) \log(\lambda), \\ \Delta\eta \rightarrow \Delta\eta - \log(\lambda). \end{aligned} \quad (9)$$

By contrast, in the LL-BFKL case that we consider for comparisons,  $\bar{\alpha}$  is *a priori* a parameter. We choose to fix it to the value 0.16 obtained in [13] by fitting the forward-jet data from the HERA accelerator at DESY, Hamburg. This unphysically small value of the coupling is indicative of the slower energy dependence of the forward-jet data

compared to the LL-BFKL cross section. And in fact, the value  $\bar{\alpha} = 0.16$  mimics the slower energy dependence of the NLL-BFKL cross section (in this case the average value of  $\bar{\alpha}$  is about 0.25), which in the forward-jet case is consistent with the data. Therefore in both cases one deals with one-parameter formulas; the absolute normalization is not under control. In the NLL case, this is due to the fact that we do not use next-to-leading order (NLO) impact factors, although the correction should be of order one.

Finally, let us point out that in general collinear and  $k_T$  factorization are two distinct schemes to factorize a hard process from a soft process (as is the case for the proton structure function  $F_2$ ), and should not be mixed. But the process we are investigating is different: it is the collinear factorization which is used to separate the hard part from the soft part, and the  $k_T$  factorization is only used within the hard part itself. This allows us to factorize it into three hard pieces: two impact factors defined order-by-order with respect to  $\alpha_s$  and the BFKL Green function where a resummation of leading (and next-to-leading) logarithms is performed.

### III. COMPARISON WITH TEVATRON DATA

The D0 collaboration has performed a measurement of the jet-gap-jet event rate as a function of the second leading jet transverse energy  $E_T = |p_T|$  and also as a function of the rapidity difference  $\Delta\eta$  between the two leading jets [1]. They requested two jets reconstructed in the D0 calorimeter with  $E_T > 15$  GeV for the second leading jet and the following cuts on the jet rapidities:  $1.9 < |\eta_{1,2}| < 4.1$  and  $\eta_1 \eta_2 < 0$ . The difference in rapidity between both jets  $\Delta\eta$  was imposed to be bigger than 4. The D0 collaboration measured the ratio of that production cross section with a gap of at least 4 units of rapidity between the jets, to the dijet inclusive cross section. The first measurement performed presented the jet-gap-jet ratio as a function of the second leading jet  $E_T$ , and the second and third measurements displayed the ratio as a function of  $\Delta\eta$  for the low- $E_T$  and high- $E_T$  jet samples, respectively (low  $E_T$  means  $15 < E_T < 25$  GeV and high  $E_T$  means  $E_T > 30$  GeV; those cuts apply to both jets).

In the following, instead of using  $x_1$  and  $x_2$  we will work with the rapidities of the two jets  $\eta_1 = \ln(x_1\sqrt{s}/E_T)$  and  $\eta_2 = -\ln(x_2\sqrt{s}/E_T)$  and with the average rapidity  $y = (\eta_1 + \eta_2)/2$ :

$$\begin{aligned} x_1 &= \frac{E_T}{\sqrt{s}} \exp(\Delta\eta/2 + y), & x_2 &= \frac{E_T}{\sqrt{s}} \exp(\Delta\eta/2 - y), \\ \frac{d\sigma^{pp \rightarrow XJJY}}{dy d\Delta\eta dE_T^2} &= x_1 x_2 \frac{d\sigma^{pp \rightarrow XJJY}}{dx_1 dx_2 dp_T^2}. \end{aligned} \quad (10)$$

For comparison with the different measurements, we integrate the NLL-BFKL cross section over  $y$  and  $\Delta\eta$ , or  $y$  and  $E_T$ , taking into account the cuts detailed above.

### A. Effect of nonzero conformal spins and NLL/LL comparison

Before comparing our BFKL calculations with the Tevatron measurements, it is worth discussing the effect of taking into account all the conformal spins at LL and NLL which was not performed up to now. In Fig. 2, we give the ratio of the different conformal-spin contributions for  $|p| = 0, 1, 2, 3$ , and 4 with respect to the sum of all components. First we see that the  $p = 0$  component dominates the cross section, which is natural since it is the only conformal spin for which  $\chi_{\text{eff}}$  is positive at the saddle point. However, the relative size of the  $|p| = 1$  contributions is large at high  $E_T$  and low  $\Delta\eta$ , where it can reach up to 30%. Indeed, for smaller values of  $\bar{\alpha}(p_T^2)\Delta\eta$  in the exponential in (4), the contribution of higher conformal spins is less suppressed. The  $E_T$  dependence of the  $|p| = 1$  contributions is also not negligible and varies between 10% to 30% for a transverse energy between 15 and 60 GeV. It is finally worth noticing that considering only the conformal spin  $p = 0$  component instead of computing the sum of all components leads in general to larger differences at LL than at NLL, especially at high  $E_T$ .

Let us now evaluate the relative NLL corrections with respect to the LL-BFKL cross section. In Fig. 3, both calculations are compared with their normalizations adjusted to describe the data (this will be discussed next), therefore the cross sections displayed on the left plots are similar. Considering the shapes of the curves, the differences between the NLL and LL calculations are in general small. This is due to the small effective value used for  $\bar{\alpha}$  in the LL calculation. However one can see on the right plots, in which the NLL/LL ratios are displayed, that the differences are sizeable in the case of the  $\Delta\eta$  dependence for high- $E_T$  jets ( $E_T > 30$  GeV).

### B. Comparison with the D0 measurement

In Fig. 4, we compare our predictions with the D0 measurements. The jet-gap-jet cross section is computed using the LL- or NLL-BFKL formalism, while the total cross section for dijets separated by a rapidity interval  $\Delta\eta$  is calculated using the NLOJet++ program [22]. To obtain the NLO QCD predictions of the dijet cross section, by which the jet-gap-jet cross section is divided, the parton-parton hard cross section is computed at next-to-leading order with respect to  $\alpha_s$ , and the leading and next-to-leading logarithms  $\alpha_s^n \log^n E_T^2$  and  $\alpha_s^n \log^{n-1} E_T^2$  are resummed using the Dokshitzer-Gribov-Lipatov-Altarelli-Parisi equations [23] which govern the evolution of the parton distribution functions of the proton. We used the CTEQ6.1M parton distribution functions [24], and the renormalization and factorization scale  $\mu_r$  and  $\mu_f$  were chosen as  $\mu_r = \mu_f = E_{T1}$ , the transverse energy of the leading jet.

It is worth pointing out that these calculations are performed at the parton level, and the hadronization effects cannot be taken into account at this stage. However, the fact that the D0 collaboration measured ratios of cross sections reduces the influence of hadronization corrections and of the choice for the jet algorithm, since most of these effects are the same for jet-gap-jet or dijet events. This is however not the case for underlying event corrections which do not play any role for jet-gap-jet events since a gap is observed. These corrections depend only smoothly on  $E_T$  and  $\Delta\eta$  in the limited  $E_T$  range of the D0 measurement, and their largest effect is taken into account in our approach with the gap-survival probability of  $S = 0.1$  at the Tevatron.

Since the normalizations of our BFKL calculations are not under control, we fit them to the D0 measurement for the jet-gap-jet cross section ratio as a function of  $E_T$ . For

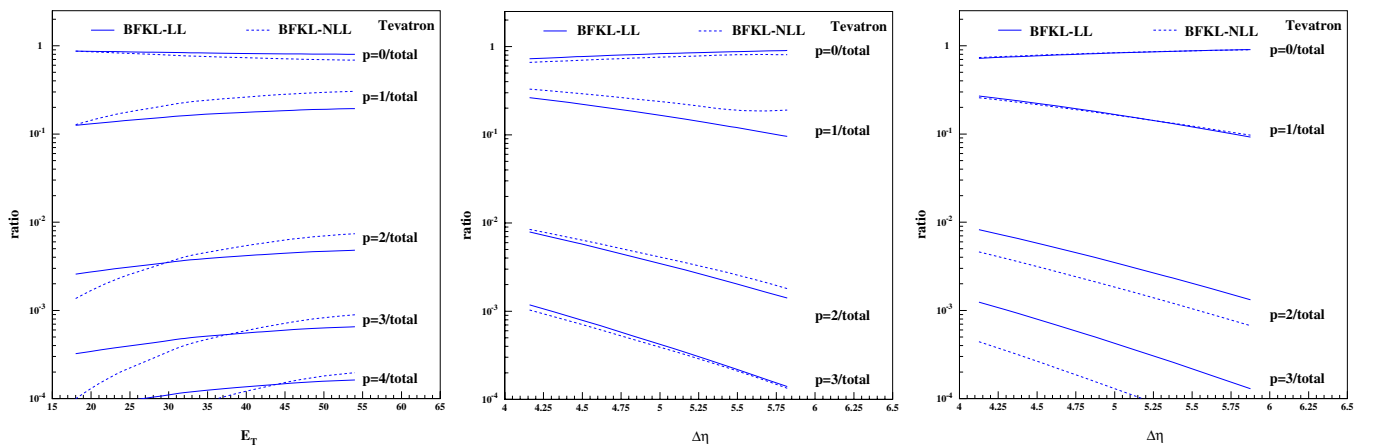


FIG. 2 (color online). Ratio between the conformal-spin components  $|p| = 0, 1, 2, 3$ , and 4, and the total BFKL cross section at LL and NLL accuracy for Tevatron kinematics. Left plot: as a function of  $E_T$  for  $\Delta\eta > 4$ ; center plot: as a function  $\Delta\eta$  for the second leading jet with  $15 < E_T < 25$  GeV; right plot: as a function  $\Delta\eta$  for the second leading jet with  $E_T > 30$  GeV. The  $|p| = 1$  contribution [meaning conformal spins 2 and  $-2$ , see (4)] becomes sizable at high  $E_T$  and low  $\Delta\eta$ .



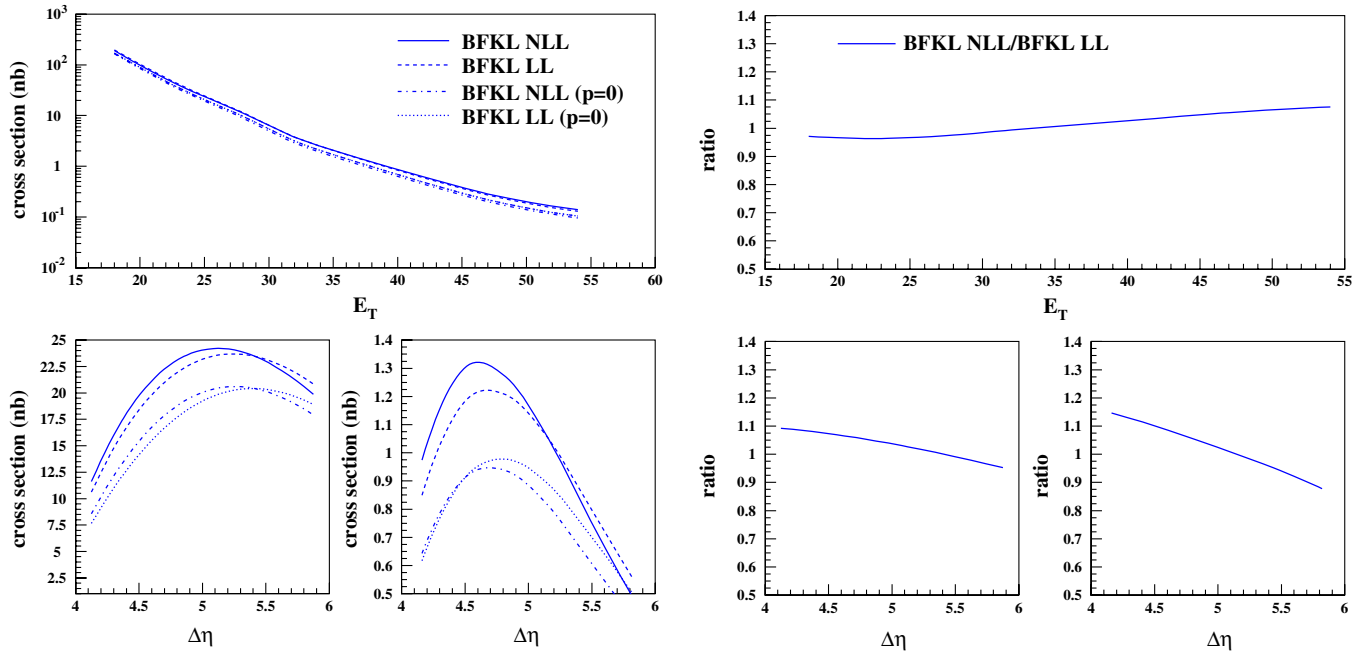


FIG. 3 (color online). Left plots: LL- and NLL-BFKL cross sections as a function of the momentum transfer  $E_T$  (upper plot) and the rapidity gap  $\Delta\eta$  (lower plots,  $15 < E_T < 25$  GeV and  $E_T > 30$  GeV); we also give the cross sections when only the conformal-spin component  $p = 0$  is included. Right plots: ratio of the NLL- and LL-BFKL calculations. Since both normalizations have been adjusted to reproduce the data, the ratios are close to 1.

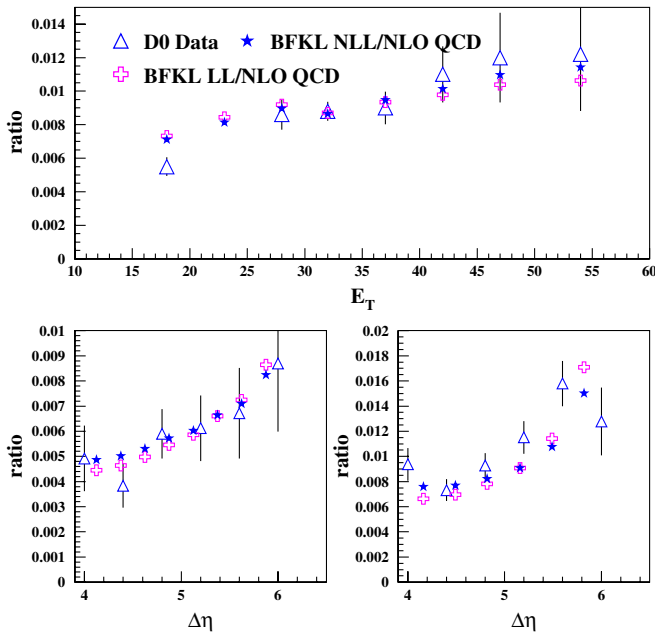


FIG. 4 (color online). Comparisons between the D0 measurements of the jet-gap-jet event ratio with the NLL- and LL-BFKL calculations. The NLL calculation is in good agreement with the data without the need to adjust the normalization. The LL calculation also gives a good description of the data after its normalization has been adjusted, although the fit shows that the NLL description is better.

the NLL-BFKL (resp. LL-BFKL) calculation, the normalization is 1.0 (0.84) with a  $\chi^2/\text{d.o.f.}$  of 0.9/6 (1.7/6) when one considers only the points with  $E_T > 25$  GeV in the fit. Interestingly enough, the normalizations are both close to 1, and our NLL-BFKL prediction with leading-order impact factors has the correct normalization and does not need to be adjusted after all. It is worth also noticing that the normalizations for the LL- and NLL-BFKL calculations are similar, while for the QCD calculation of the jet cross section, this is not the case when both jets are separated by an interval in rapidity larger than 4. In fact the NLO QCD result is about 20 times larger than the LO one, and it would be useful to know the QCD cross section at next-to-next-to-leading order to check if the higher order corrections are still large.

The resulting jet-gap-jet cross section ratios are displayed in the upper plot of Fig. 4. We notice that the  $E_T$  dependence of the cross section is well described, with the exception of the lowest  $E_T$  point where the measurement is lower than our calculation (this is why we did not include it in the fit to compute the normalization). This lowest  $E_T$  point is definitely more sensitive to hadronization or underlying event corrections, and this might be the reason why it is poorly described. We use the same normalizations to predict the rapidity dependence of the jet-gap-jet cross section ratio for the low- and high- $E_T$  samples, and the result is shown on the lower plots of Fig. 4. We also notice a good agreement between our calculations and the D0 measurement, without any further adjustment of the normalizations. This is a powerful result, the NLL-BFKL

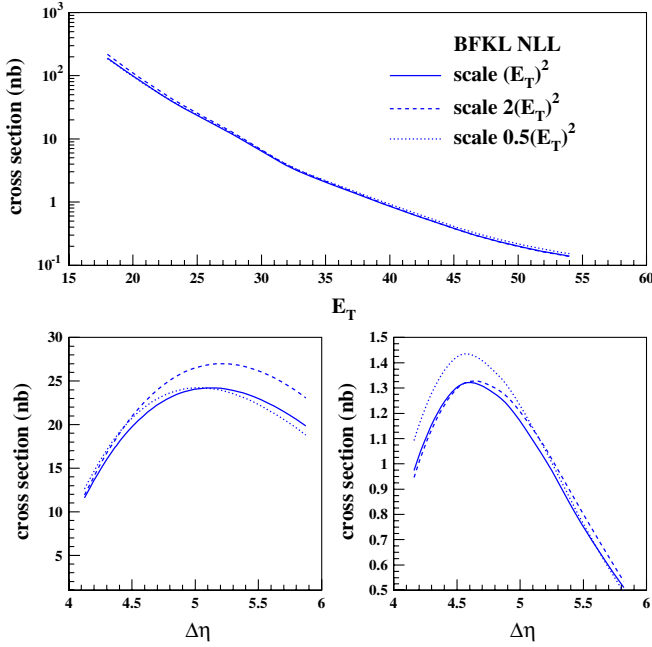


FIG. 5 (color online). Renormalization scale dependence of the NLL-BFKL calculations for the D0 measurements. The scale uncertainty is evaluated by modifying the  $E_T^2$  scale used by default to  $E_T^2/2$  or  $2E_T^2$ . The effect is of the order of 10%–15%.

prediction has the correct normalization for the three measurements. In Fig. 5, we show the scale dependence of the NLL-BFKL calculations; the uncertainty is evaluated by modifying the  $E_T^2$  scale used by default to  $E_T^2/2$  or  $2E_T^2$ .

The uncertainty of the predictions is of the order of 10%–15%.

The fact that the LL-BFKL cross section is in good agreement with the data when a fixed value of the coupling is considered is consistent with the results of [5]. The fit performed on the data as a function of  $E_T$  showed that including NLL corrections in the BFKL framework improves the description of the data. This is also consistent with the findings of [6], where some NLL corrections were effectively included in a numerical way. In this study we confronted for the first time predictions obtained with the full analytic expression of the NLL-BFKL kernel to the Tevatron data, and the result is satisfactory.

#### IV. PREDICTIONS FOR THE LHC

Using the normalizations obtained from the fits to the D0 data, we are able to predict the cross sections at the LHC. In doing so, we also have to change the gap-survival probability from 0.1, the value used for the Tevatron, to 0.03, the proper value for the LHC. The values of the NLL-BFKL cross sections are shown in Fig. 6 as a function of  $E_T$  for different  $\Delta\eta$  ranges and in Fig. 7 as a function of  $\Delta\eta$  for different  $E_T$  ranges. In both figures, the cross sections are displayed on the left plots, and on the right plots they are divided by the NLOJet++ prediction for the inclusive dijet cross section. In Fig. 8, we display the scale dependence of the NLL-BFKL calculations (the uncertainty is obtained by modifying the default  $E_T^2$  scale to  $E_T^2/2$  or  $2E_T^2$ ) as a function of the  $\Delta\eta$  between the two jets.

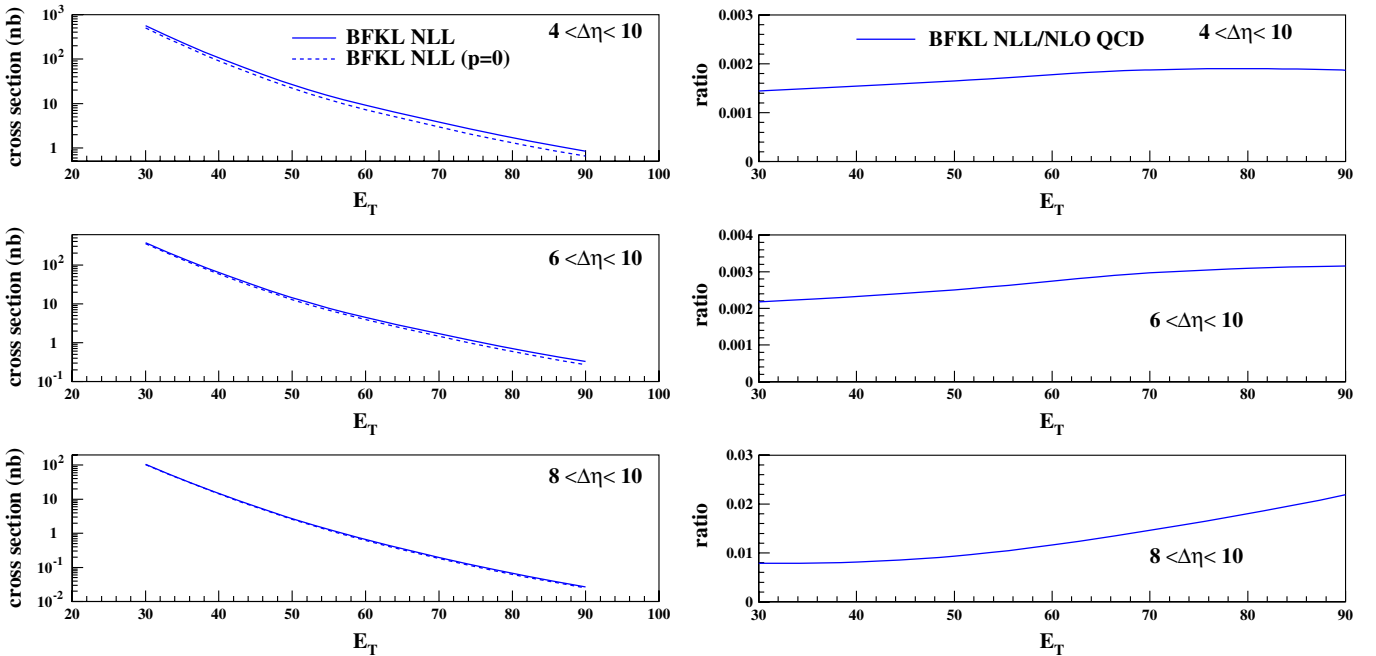


FIG. 6 (color online). Left plot: NLL-BFKL jet-gap-jet cross section as a function of  $E_T$  for three different regions in  $\Delta\eta$  at the LHC. Right plot: the left-plot curves are divided by the NLO QCD dijet inclusive cross section.

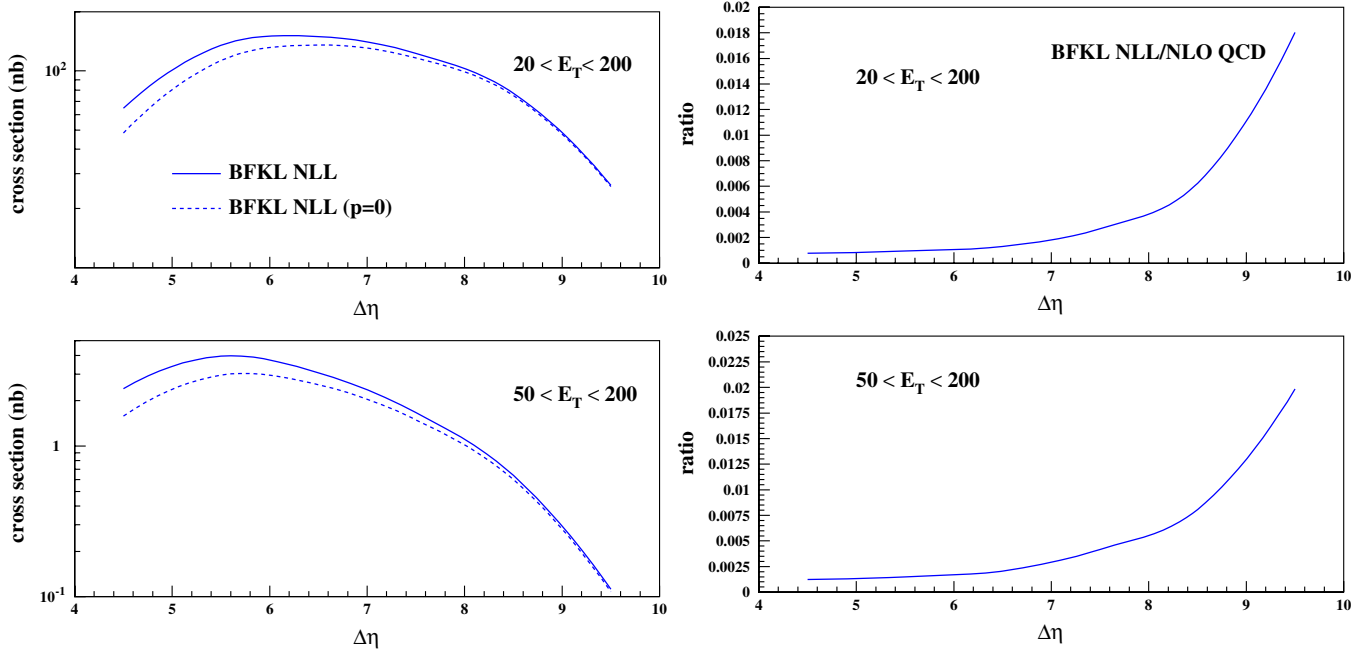


FIG. 7 (color online). Left plot: NLL-BFKL jet-gap-jet cross section as a function of the rapidity gap  $\Delta\eta$  for two different  $E_T$  regions at the LHC. Right plot: the left-plot curves are divided by the NLO QCD dijet inclusive cross section.

The uncertainty of the predictions is of the order of 10%–20% (and is roughly the same as a function of  $E_T$ ).

Comparing the relative contributions from the different conformal-spin components, we could see that the  $|p| = 1$  and  $|p| = 2$  contributions are large at small  $\Delta\eta$  and at

large  $E_T$ , and they cannot be neglected as is shown in Fig. 9. At large  $\Delta\eta$  and low  $E_T$ , the  $p = 0$  component is by far the largest one. Also, it can be noticed that the cross section is high enough to be measured at the LHC in special runs, collecting integrated luminosities of a few  $100 \text{ pb}^{-1}$ . Nevertheless, a good energy calibration will be needed to deal with not so energetic jets which are in addition quite forward. Finally, a clear prediction is that the percentage of the jet-gap-jet events is higher when the interval in rapidity between the two jets  $\Delta\eta$  is large.

## V. CONCLUSIONS

Within the BFKL framework at NLL accuracy, we have investigated diffractive events in hadron-hadron collisions in which two high- $E_T$  jets are produced and separated by a large rapidity gap  $\Delta\eta$ . Using renormalization-group improved NLL kernels in the S4 scheme, the NLL-BFKL effects were taken into account through the effective kernel obtained from the implicit Eq. (7). We implemented the MT prescription to couple the BFKL Pomeron to colored impact factors, and this allowed our phenomenological study of NLL-BFKL effects in jet-gap-jet events. We point out that we used only leading-order impact factors, and the implementation of the NLO impact factors goes beyond the scope of our phenomenological analysis. Finally, dividing our jet-gap-jet BFKL calculations by the NLO QCD predictions for the inclusive dijet cross section, we showed that the BFKL predictions were in good agreement with the Tevatron data for both the  $E_T$  and  $\Delta\eta$  dependence of the jet-gap-jet cross section ratios. In the case of the NLL

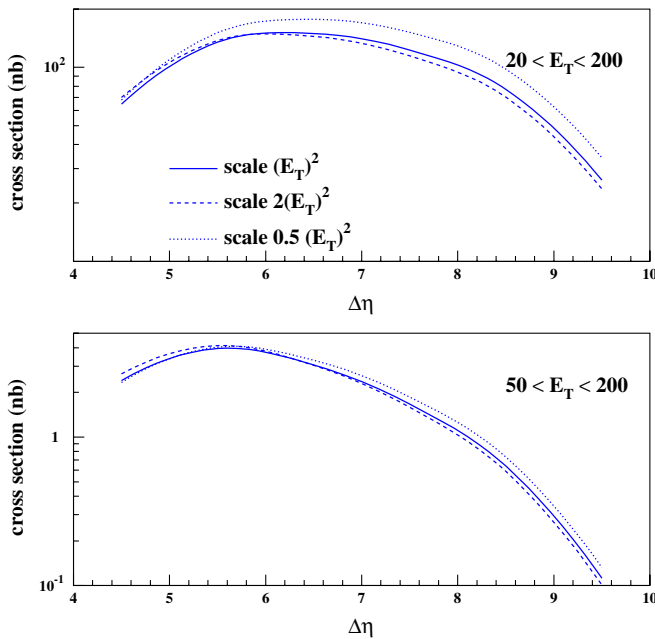


FIG. 8 (color online). Renormalization scale dependence of the NLL-BFKL calculations for the LHC. The scale uncertainty is evaluated by modifying the  $E_T^2$  scale used by default to  $E_T^2/2$  or  $2E_T^2$ . The effect is of the order of 10%–20%.

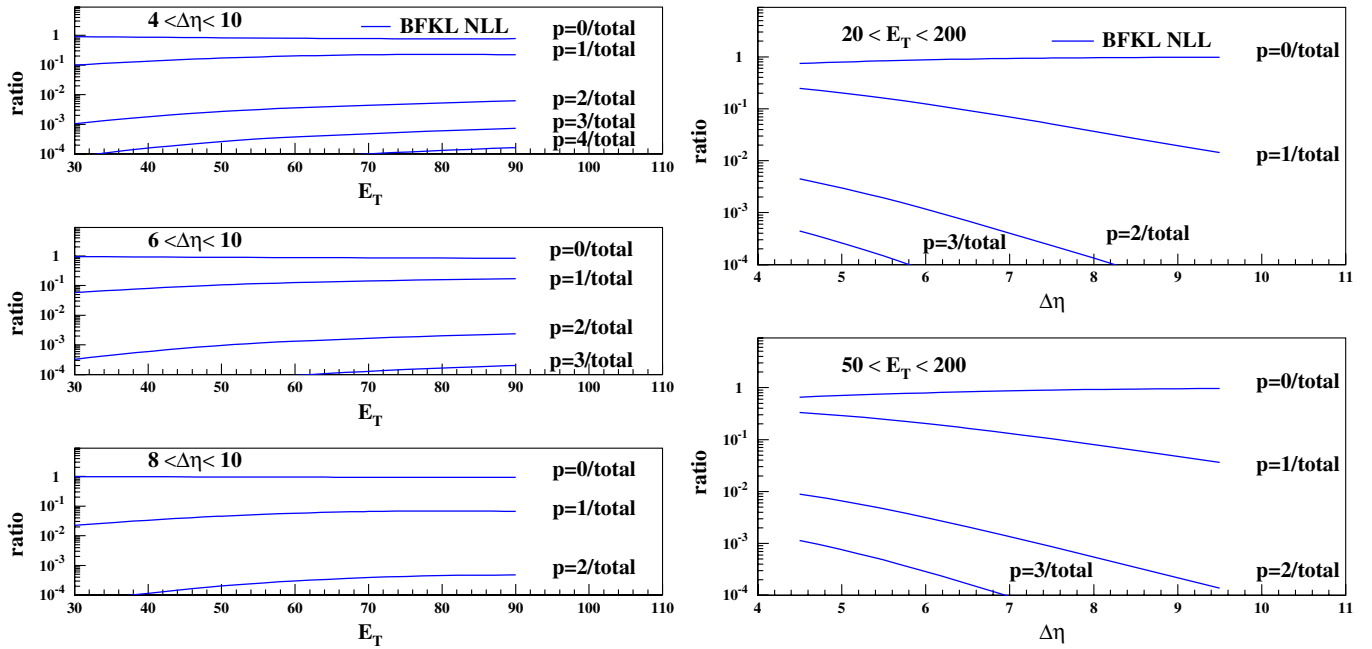


FIG. 9 (color online). Ratio between the conformal-spin components  $|p| = 0, 1, 2, 3$ , and  $4$  and the total BFKL cross section at NLL accuracy for LHC kinematics. Left plot: as a function of  $E_T$  in different regions of  $\Delta\eta$ ; right plots: as a function  $\Delta\eta$  for a leading jet with  $20 < E_T < 200$  GeV or  $50 < E_T < 200$  GeV.

calculation, adjusting the normalization was not needed for any of the three measurements.

The LL-BFKL predictions can also describe the data with the fixed value of the coupling  $\bar{\alpha} = 0.16$  and a normalization factor of order one. Still the better description was obtained with the NLL formulation. We presented predictions which could be tested at the LHC, for the same jet-gap-jet event ratio measured at the Tevatron, but

for larger rapidity gaps which can be obtained at the LHC. This should provide a strong test of the BFKL regime.

## ACKNOWLEDGMENTS

C. M. is supported by the European Commission under the FP6 program, Contract No. MOIF-CT-2006-039860.

- 
- [1] B. Abbott *et al.* (D0 Collaboration), Phys. Lett. B **440**, 189 (1998); F. Abe *et al.* (CDF Collaboration), Phys. Rev. Lett. **80**, 1156 (1998).
  - [2] L. N. Lipatov, Sov. J. Nucl. Phys. **23**, 338 (1976); E. A. Kuraev, L. N. Lipatov, and V. S. Fadin, Sov. Phys. JETP **45**, 199 (1977); I. I. Balitsky and L. N. Lipatov, Sov. J. Nucl. Phys. **28**, 822 (1978).
  - [3] L. N. Lipatov, Sov. Phys. JETP **63**, 904 (1986).
  - [4] A. H. Mueller and W. K. Tang, Phys. Lett. B **284**, 123 (1992).
  - [5] B. Cox, J. R. Forshaw, and L. Lonnblad, J. High Energy Phys. **10** (1999) 023.
  - [6] R. Enberg, G. Ingelman, and L. Motyka, Phys. Lett. B **524**, 273 (2002).
  - [7] B. Andersson, G. Gustafson, H. Kharraziha, and J. Samuelsson, Z. Phys. C **71**, 613 (1996); J. Kwiecinski, A. D. Martin, and P. J. Sutton, Z. Phys. C **71**, 585 (1996).
  - [8] V. S. Fadin and L. N. Lipatov, Phys. Lett. B **429**, 127 (1998); M. Ciafaloni, Phys. Lett. B **429**, 363 (1998); M. Ciafaloni and G. Camici, Phys. Lett. B **430**, 349 (1998).
  - [9] G. P. Salam, J. High Energy Phys. **07** (1998) 019.
  - [10] M. Ciafaloni, D. Colferai, and G. P. Salam, Phys. Rev. D **60**, 114036 (1999); J. High Energy Phys. **10** (1999) 017.
  - [11] S. J. Brodsky, V. S. Fadin, V. T. Kim, L. N. Lipatov, and G. B. Pivovarov, JETP Lett. **70**, 155 (1999); R. S. Thorne, Phys. Rev. D **60**, 054031 (1999); G. Altarelli, R. D. Ball, and S. Forte, Nucl. Phys. **B621**, 359 (2002).
  - [12] R. B. Peschanski, C. Royon, and L. Schoeffel, Nucl. Phys. **B716**, 401 (2005).
  - [13] O. Kepka, C. Royon, C. Marquet, and R. B. Peschanski, Phys. Lett. B **655**, 236 (2007); Eur. Phys. J. C **55**, 259 (2008).
  - [14] A. Sabio Vera and F. Schwennsen, Phys. Rev. D **77**, 014001 (2008).
  - [15] C. Marquet and C. Royon, Phys. Rev. D **79**, 034028 (2009).



- [16] A. Sabio Vera, Nucl. Phys. **B746**, 1 (2006); A. Sabio Vera and F. Schwennsen, Nucl. Phys. **B776**, 170 (2007).
- [17] J. Bartels, J.R. Forshaw, H. Lotter, L.N. Lipatov, M.G. Ryskin, and M. Wusthoff, Phys. Lett. B **348**, 589 (1995); J. Bartels, L.N. Lipatov, M. Salvadore, and G.P. Vacca, Nucl. Phys. **B726**, 53 (2005).
- [18] L. Motyka, A.D. Martin, and M.G. Ryskin, Phys. Lett. B **524**, 107 (2002).
- [19] A.V. Kotikov and L.N. Lipatov, Nucl. Phys. **B582**, 19 (2000); **B661**, 19 (2003); **B685**, 405(E) (2004).
- [20] V.S. Fadin, R. Fiore, M.I. Kotsky, and A. Papa, Phys. Rev. D **61**, 094006 (2000); **61**, 094005 (2000).
- [21] Y.V. Kovchegov and A.H. Mueller, Phys. Lett. B **439**, 428 (1998); M. Ciafaloni, D. Colferai, G.P. Salam, and A.M. Stasto, Phys. Rev. D **68**, 114003 (2003).
- [22] Z. Nagy and Z. Trocsanyi, Phys. Rev. Lett. **87**, 082001 (2001).
- [23] G. Altarelli and G. Parisi, Nucl. Phys. **B126**, 298 (1977); V.N. Gribov and L.N. Lipatov, Sov. J. Nucl. Phys. **15**, 438 (1972); **15**, 675 (1972); Y.L. Dokshitzer, Sov. Phys. JETP **46**, 641 (1977).
- [24] J. Pumplin, D.R. Stump, J. Huston, H.L. Lai, P.M. Nadolsky, and W.K. Tung, J. High Energy Phys. 07 (2002) 012.